JOURNAL OF AIRCRAFT
Vol. 32, No. 5, September–October 1995

Application of an Artificial Neural Network as a Flight Test Data Estimator

Roger L. McMillen*
Raytheon Aircraft Company, Wichita, Kansas 67201-0085
and
James E. Steck† and Kamran Rokhsaz‡
Wichita State University, Wichita, Kansas 67260-0044

During a flight test program, certain instrumented parameters are subject to degradation due to wear and tear. Over the course of a flight test program, data from several flights will be lost due to undetected instrumentation faults. The application of artificial neural networks as flight test data estimators has been proposed with the intention of reducing the aforementioned cost and wasted test flights. Several network topologies have been studied. A simulation program has been used to identify the appropriate network topology for this task. It is shown that a single network is not capable of predicting all of the correct values of the suspect parameters based solely on the information received from the reliable instruments. However, it is shown that a collection of smaller networks can succeed in this task, with each network predicting one suspect parameter. Limited training and test results based on simulation-generated data are presented. Actual flight test data from a typical business jet have been used to verify this concept and these results are presented as well. It is demonstrated that in most cases these networks are capable of predicting the measured parameter outputs with sufficient accuracy to enable identification of instrumentation system degradation.

Nomenclature

C_L, C_D, C_Y = lift, drag, and side force coefficients
C_l, C_M, C_n = rolling, pitching, and yawing moment coefficients
$\bar{c}$ = mean aerodynamic chord
b = wingspan
$f(x)$ = neural network activation function
p, q, r = roll, pitch, and yaw rates
u, v, w = velocity components along each of the axes
x, y, z = body axes
α = angle of attack
β = sideslip angle
δ_A, δ_e, δ_R = aileron, elevator, and rudder deflection angles
Θ = pitch angle
Φ = bank angle

Subscripts
B = body axes
ELEV = due to elevator
GEAR = due to landing gear
S = stability axes
SPOIL = due to spoiler
STAB = due to stabilizer
W = due to wing
0 = aerodynamic quantity at zero angle of attack

Superscript
$\hat{}$ = nondimensional roll, pitch, and yaw rates

I. Introduction

OVER the past decade the study and utilization of artificial neural networks (ANNs) has steadily expanded. The range of practical applications for these networks is indicated by the breadth of studies that have grown out of such diverse backgrounds as biology, computer science, psychology, and statistics. This growth is especially evident in the aerospace community where a wide variety of applications have been explored. ANNs have found applications in almost every field of study. What follows is a brief survey primarily concerned with studies conducted in the aerospace engineering field.

The identification and control of uncertain and/or highly nonlinear plants has been an area of significant activity in the study and application of ANNs. The problem of system identification, which is one of the issues central to this article, is addressed in Refs. 1–3. Also, a range of applications in which ANNs have been utilized in aerospace engineering have been presented in Refs. 4–14. Many of the applications cited in these references provided insight into the capabilities of ANNs for identifying and controlling highly nonlinear systems without the need for structured modeling of the system a priori. In particular, Ref. 9 dealt with the automated screening of propulsion data from the Space Shuttle main engine. The problem addressed in this reference is similar to the research in the current study. However, the unstructured nature of the ANNs in modeling the aircraft aerodynamics identified in Refs. 11 and 12 and the potential for their use in screening flight data proposed in Ref. 14 provided the direct impetus for conducting the current research project.

The current study expands the possible uses of ANNs into another area of aerospace data analysis. Its purpose is to apply ANNs to the health monitoring of a flight test instrumentation package. During the course of a flight test program the flight test instrumentation package must continually be monitored to ensure the validity of the acquired data. As a flight program progresses, certain instrumented parameters are subject to degradation. Angle of attack and sideslip vanes are particularly susceptible to damage. Many of these parameters cannot be properly evaluated during a normal preflight by the in-

Received Nov. 17, 1994; revision received April 9, 1995; accepted for publication April 13, 1995.

*Group Engineer, Guidance and Control. Senior Member AIAA.
†Assistant Professor, Mechanical Engineering. Senior Member AIAA.
‡Assistant Professor, Aerospace Engineering. Associate Fellow AIAA.

strumentation engineer. They can only be checked during a review of the flight data. The time spent assessing the instrumentation veracity may seem unproductive to the flight data analyst, however, this is necessary if schedule delays and budget overruns due to lost flight data are to be minimized. If an automated system could be implemented to relieve the data analyst of the majority of this tedium, then the likelihood of detecting instrumentation degradation could be greatly increased and the data analyst's time would become more productive. Furthermore, use of such a system during an ongoing flight test program would reduce the number of wasted flights due to undetected instrumentation faults.

It is the objective of this research to study the feasibility of developing such a system. The proposed system would implement ANNs to map the trusted input parameters to the parameters likely to degrade over the life of a flight program.

II. Method of Analysis

The intent of this research, as stated earlier, was to develop ANNs for the identification of flight test instrumentation degradation over the course of a test program. To this end, the following strategy was outlined:

1) Train a series of candidate networks using I/O pairs generated from the solution of the six-degree-of-freedom equations of motion for a typical business jet. These data, without noise or uncertainty, would be used to identify and select the proper network topology.

2) Identify the most suitable network topology based on overall performance and generalization capability. Global least-squares-error minimization, generalization to inputs outside the test range, and training time for the network would be used as measures of network performance.

3) Train and test the selected network on flight test data from a typical business jet. Also, test characterization and generalization using data with noise and uncertainty in the measurements.

Throughout this work, all flight data utilized were generated from steady maneuvers; specifically those typical of an executive business jet. Therefore, extreme nonlinear maneuvers were not considered. The use of steady maneuvers was intentional and was not a limitation of the current research. Application of this approach to high-performance aircraft, such as fighters, may require re-evaluation of the modeling technique. The details of the current approach are described in the following sections.

A. Neural Network

For a more comprehensive background involving ANN, the reader is advised to consult Ref. 15. A very brief summary of the material in that document is presented here.

Figure 1 shows the schematic of the ANNs used here. This was a feed-forward network in which each layer was fully connected to the following layer. This network utilized the delta rule for back-propagation learning based on the global network error. The initial problem formulation consisted of a single network into which all trusted parameters were input and from which all suspect parameters were output. The input layer had 12 neurons, one for each of those flight test parameters that were reliable and least susceptible to degradation over the duration of the flight test program. In terms of the equations of motion, these 12 parameters could be used to uniquely define the state of the aircraft over all the maneuvers of interest. In the final network topology, the output layer of each network consisted of one neuron for the suspect parameter. The input layer, employing linear activation functions, was connected to two hidden layers, each using hyperbolic tangent activation functions of the form

$$f(x) = (e^x - e^{-x})/(e^x + e^{-x}) \tag{1}$$

All neurons were connected with simple multiplicative weighted connections. The output signal of the ith neuron was given in terms of the sum of the signals from neurons j, weighted by w_{ij}, as

$$x_i = f\left(\sum_j w_{ij}x_j\right) \tag{2}$$

where f_i is the activation function of neuron i. The neuron of the output layer employed linear activation functions.

The network was trained by presenting it with a multitude of training pairs. Each pair consisted of input data for the network and correct network output. Correct output values were collected either from simulation or from flight test data validated by hand. The inputs to the network were the values of those parameters that were considered least susceptible to degradation during the flight test program. The network was trained on pairs of inputs and correct outputs and a comparison was made between the correct outputs and the network outputs to determine the ability of the network to learn the required mapping. Convergence was assumed when global error between the network output and the correct output decreased to a prescribed value. The network was then presented with inputs for those cases that were absent in the training domain. Comparison of the network outputs with the actual values was used to quantify generalization. Different combinations of processing element architecture were then tried in the two hidden layers to complete a series of network topologies for testing.

B. Equations of Motion

In order to use ANNs in the flight data review process, a unique I/O relationship had to be established between the measured parameters that were considered less susceptible to damage or degradation during a flight test program and those that were likely to develop problems. Based on experience with past flight test programs the data illustrated in Table 1 were chosen and divided into trusted vs suspect categories.

The first step in the process of developing the ANN was to choose the network type and topology with which to solve the aircraft system identification problem. To eliminate the

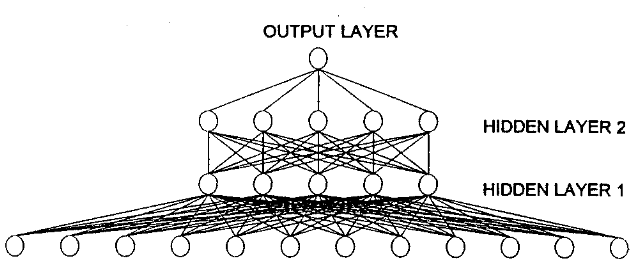

Fig. 1 Schematic of a fully connected feed-forward ANN.

Table 1 Flight test data parameters

Trusted parameters	Suspect parameters
Weight	Angle of attack
c.g.	Sideslip angle
Airspeed	Stabilizer incidence
Altitude	Aileron deflection
Outside air temperature	Spoiler deflection
Longitudinal acceleration	Rudder deflection
Lateral acceleration	Pitch attitude
Vertical acceleration	Bank angle
Pitch rate	
Roll rate	
Yaw rate	
Turbine rpm - N1	

added complexity of instrumentation noise and measurement uncertainty during the selection of an appropriate network topology, a set of "perfect" I/O pairs was required. A detailed six-degree-of-freedom simulation was created in order to provide these perfect pairs. These equations formed the basis of the simulation program written to generate the perfect training pairs used for ANN training and testing. All accelerations were set to zero and the total mass and the location of the aircraft c.g. were assumed to be fixed. This reduced the equations of motion to a set of algebraic expressions. The derivation and simplification of the equations of motion were verified with Refs. 16 and 17.

The aerodynamic model for this simulation was kept relatively simple, though the simulation itself was capable of handling any degree of nonlinearity. The aerodynamic coefficients were modeled in the standard Taylor series format in the stability axis system. The specific form of the aerodynamic coefficients is presented in Eqs. (3–8):

$$C_L = C_{L_0} + C_{L_\alpha}\alpha + (C_{M_{\mathrm{STAB}}} + C_{M_{\mathrm{ELEV}}})(-\bar{c}_W/L_H) + C_{L_q}\hat{q} + C_{L_{\dot{\alpha}}}\hat{\dot{\alpha}} \tag{3}$$

$$C_D = C_{D_0} + \left(\frac{\partial C_D}{\partial C_L^2}\right) C_L^2 + C_{D_{\mathrm{STAB}}} \tag{4}$$

$$C_M = C_{M_0} + C_{M_\alpha}\alpha + C_{M_{\mathrm{STAB}}} + C_{M_{\mathrm{ELEV}}} + C_{M_q}\hat{q} + C_{M_{\dot{\alpha}}}\hat{\dot{\alpha}} + (C_L \cos\alpha + C_D \sin\alpha)(\bar{x}_{\mathrm{c.g.}} - 0.25) + (C_L \sin\alpha - C_D \cos\alpha)[(Z_{AC} - Z_{\mathrm{c.g.}})/\bar{c}_W] \tag{5}$$

$$C_l = C_{l_0} + \left(\frac{\partial C_{l_0}}{\partial \alpha}\right)\alpha + \left[C_{l_\beta} + \left(\frac{\partial C_{l_\beta}}{\partial \alpha}\right)\alpha\right]\beta + C_{l_{\delta A}}\delta_A + C_{l_{\delta \mathrm{SPOIL}}}\delta_{\mathrm{SPOIL}} + \left[C_{l_{\delta R}} + \left(\frac{\partial C_{l_{\delta R}}}{\partial \alpha}\right)\alpha\right]\delta_R + C_{l_p}\hat{p} + C_{l_r}\hat{r} \tag{6}$$

$$C_n = C_{n_0} + \left(\frac{\partial C_{n_0}}{\partial \alpha}\right)\alpha + (C_{n_\beta} + \Delta C_{n_{\beta_{\mathrm{GEAR}}}})\beta + C_{n_{\delta A}}\delta_A + \left[C_{n_{\delta \mathrm{SPOIL}}} + \left(\frac{\partial C_{n_{\delta \mathrm{SPOIL}}}}{\partial \alpha}\right)\alpha\right]\delta_{\mathrm{SPOIL}} + C_{n_{\delta R}}\delta_R + \left[C_{n_p} + \left(\frac{\partial C_{n_p}}{\alpha}\right)\alpha\right]\hat{p} + \left[C_{n_r} + \left(\frac{\partial C_{n_r}}{\partial \alpha}\right)\alpha\right]\hat{r} + C_Y(\bar{x}_{\mathrm{c.g.}} - 0.25)\left(\frac{\bar{c}_W}{b_W}\right) \tag{7}$$

$$C_Y = C_{Y_0} + C_{Y_\beta}\beta + C_{n_R}\left(\frac{-b_W}{L_V}\right) + \left[C_{Y_p} + \left(\frac{\partial C_{Y_p}}{\partial \alpha}\right)\alpha\right]\hat{p} + C_{Y_r}\hat{r} \tag{8}$$

In order to employ the previous coefficients into the equations of motion, they were transformed first into the body axes by

$$\begin{Bmatrix} C_X \\ C_Y \\ C_Z \end{Bmatrix} = \begin{bmatrix} -\cos\alpha & 0 & \sin\alpha \\ 0 & 1 & 0 \\ -\sin\alpha & 0 & -\cos\alpha \end{bmatrix} \begin{Bmatrix} C_D \\ C_Y \\ C_L \end{Bmatrix} \tag{9}$$

$$\begin{Bmatrix} C_{l_B} \\ C_{M_B} \\ C_{n_B} \end{Bmatrix} = \begin{bmatrix} \cos\alpha & 0 & -\sin\alpha \\ 0 & 1 & 0 \\ \sin\alpha & 0 & \cos\alpha \end{bmatrix} \begin{Bmatrix} C_{l_S} \\ C_{M_S} \\ C_{n_S} \end{Bmatrix} \tag{10}$$

The resulting body axis coefficients were then multiplied by the appropriate characteristic areas, lengths, and dynamic pressure and summed with thrust forces and moments. The moments generated by spinning rotors were included in this summation to accommodate those configurations with significant angular momentum from propellers or other rotating devices.

C. Flight Test Data

The data for this research originated from an extensive flight test program on a typical business jet. The complete data, in final form presented to the ANNs, are listed in Ref. 15.

Data files from 11 flights spread throughout the test program were examined to obtain reliable data for steady level flight trims, steady heading sideslips, and maneuvering stability flight conditions. These maneuvers were chosen as representatives for instrumentation checkout during a test program. Altogether, 82 training pairs and 21 test pairs were identified as reliable data points for network training and testing. Each test condition consisted of between 5–25 s of steady-state conditions over which the data were averaged. Initial aircraft weight and c.g. from a preflight weighing were summed with fuel consumed, computed from fuel totalizer readings, to arrive at a weight for each test point. Center of gravity remained essentially constant for a given flight and, therefore, was input from the flight data card. Spoiler deflection, aileron deflection, and gas turbine speed used here were computed average values rather than individual left and right inputs to the ANNs. To preclude possible corruption of the data due to data processing errors, raw angle of attack and sideslip angle from the boom-mounted vanes were used with the ANNs rather than those computed using in-flight calibrations and angular rate corrections. Similarly, outputs from the three axis accelerometer components were utilized without applying corrections for location relative to the c.g. After successful training, all these corrections would ultimately be implicitly included in the ANN weight matrices.

III. Results and Discussion

A. Simulation and Network Topology

The training data developed from the solution of the equations of motion were based on a typical set of test points likely to be obtained from a flight program. This is as opposed to designing a set of test conditions that would result in a uniform distribution of I/O pairs over the flight domain. These solutions covered a variety of steady-state maneuvers. A set of 150 flight conditions was chosen for training along with 28 for testing the network. All cases were trimmed for steady-state flight generating the pairs consisting of 12 inputs and 8 outputs for training and testing the network.

Initially, it was intended to use one network, with 12 inputs and all 8 suspect variables as the output. The results provided by this network were promising, but mixed. The network would learn the overall patterns of most parameters, but the amount of deviation around the best fit of the data was unacceptable. In addition, some parameters such as sideslip angle were not well characterized by the network. As a next step, more training pairs were generated with which to provide the sideslip angle relationship. The effect of introducing the additional pairs was to weight the sideslip conditions more heavily in the training data set. The network results after training with the revised I/O pairs showed an improvement in the characterization of sideslip angle, but the deviation on all parameters was still unacceptable. Without better identification of the system the method would not provide a useful tool for instrumentation monitoring.

The network topology was changed with the intent of reducing both the complexity of the system identification task and the training time involved in network development.

Table 2 Relative performance for angle-of-attack networks

Network topology	Training cycles	Global error	Internalization capability	Predictive capability
12-20-20-1	36,000	0.002	Excellent	Good
12-5-5-1	29,800	0.0002	Excellent	Good
12-5-2-1	45,200	0.005	Good	Good
12-2-2-1	10,900	0.0004	Fair	Fair

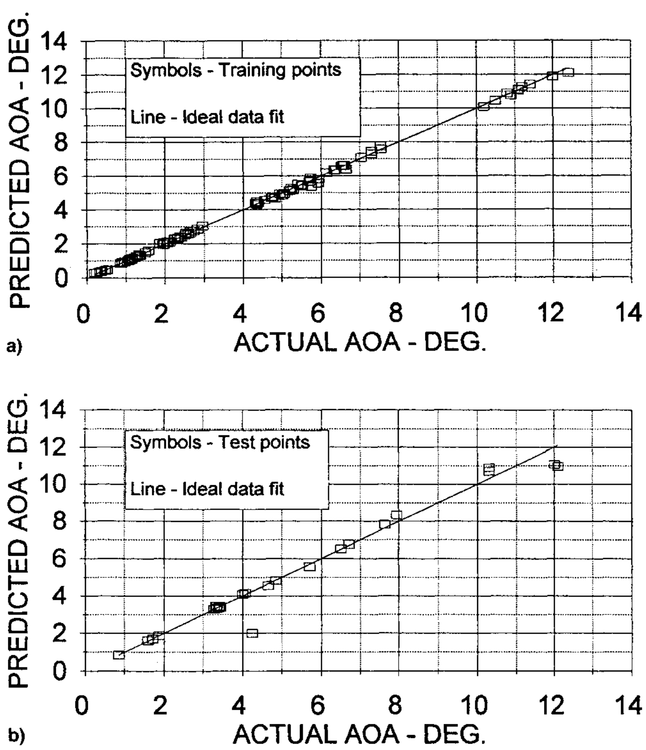

Fig. 2 a) Training and b) test results from the network for angle of attack (network topology 12-5-5-1).

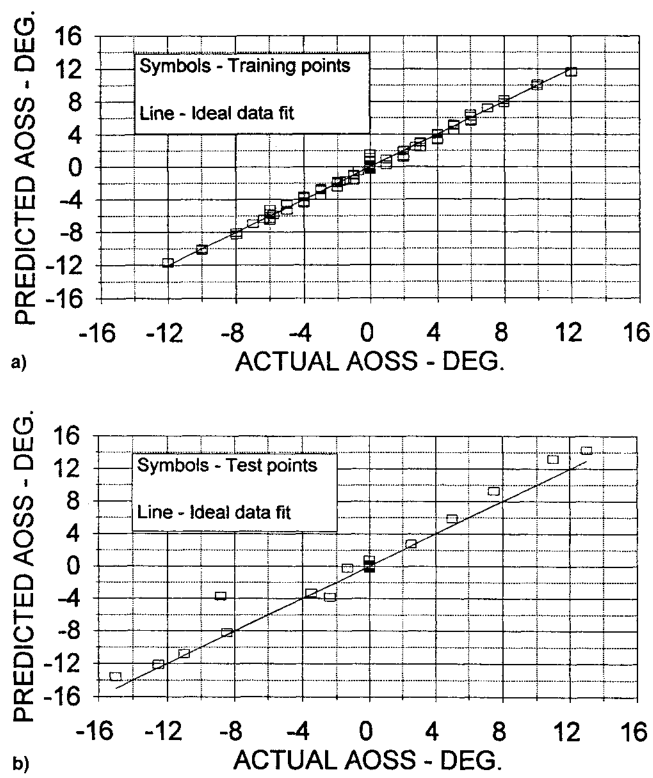

Fig. 3 a) Training and b) test results from the network for sideslip angle (network topology 12-5-5-1).

The decision was made to utilize all 12 inputs and 2 hidden layers, as before, but to require only 1 output per network. This implied using eight networks, but with fewer elements per network than the original. Of the eight networks, the parameter chosen for initial training was angle of attack. Four networks were constructed for the angle-of-attack system identification task. These networks possessed the topologies 12-20-20-1, 12-5-5-1, 12-2-2-1, and 12-2-5-1. Table 2 reflects individual network performance in terms of cycles to achieve a given global error. Internalization (how well it mapped the training data set) and prediction (how well it used this mapping to estimate outputs for the test data set) capabilities are also shown in this table. These results are based on the authors' opinion after having carefully studied the networks' performance. Figures 2a and 2b show the outcome of training as well as the test of the 12-5-5-1 network for angle of attack. Figure 2b clearly indicates the ability of the network to generalize the angle of attack for a wide range of maneuvers.

The ANN for identification of sideslip angle was created and trained next. Two networks were chosen for training and testing, a 12-20-20-1 network topology and a 12-5-5-1 network topology. Both of the networks tested for sideslip angle rapidly converged to a small global error and then stabilized. The 12-20-20-1 network trained to an error of 0.002 after 36,000 training passes and the 12-5-5-1 network to a global error of 0.003 in 58,750 training cycles. The performance of the two networks in characterizing the data was roughly equivalent. Figures 3a and 3b show the training results as well as the test results for this case. Again, these figures clearly show the ability of the network to learn the behavior of the sideslip angle. Based on the previous results, the network topology of 12-5-5-1 was chosen for system identification on the remaining 6 output parameters (i.e., stabilizer incidence, aileron deflection, spoiler deflection, rudder deflection, bank angle, and pitch attitude). For detailed results, the reader is encouraged to consult Ref. 15. In most cases the 12-5-5-1 topology provided adequate parameter identification utilizing few training passes with a relatively small network. The exceptions were spoiler, rudder, and aileron deflections. A probable cause of this was the weighting of training towards the zero sideslip conditions where spoiler and rudder were near neutral. Also, in the case of aileron deflection, the poor performance of the network was explainable. The simulation modeled a perfectly symmetric aircraft and the ailerons were used only as trim devices on this aircraft. Therefore, ailerons were almost never deflected away from neutral and the network was not able to generate a relationship between aileron deflection and the trusted input parameters.

Based on the previous results, the 12-5-5-1 topology was deemed to possess acceptable learning and generalization capabilities for the next phase of this research. This phase involved application of flight test data to test the method developed from simulation results.

B. Flight Test Results

The ANN topology chosen based on the simulation results was now used for all flight test data. Table 3 summarizes the results of training and testing. It should be stated at this point that the ANNs for modeling of lateral-directional parameters

Table 3 Results of flight test network training

Suspect parameter	Training cycles	Global error	Capability to predict system degradation
Angle of attack	66,000	0.004	Adequate for most problems, needs further refinement to predict subtle degradation
Sideslip angle	99,000	0.0075	Additional training data in the moderate to high sideslip range is required for conclusive results
Stabilizer incidence	42,200	0.01	Excellent for predicting any level of degradation
Aileron deflection	56,000	0.02	Capable of identifying any degree of degradation
Spoiler deflection	74,500	0.0025	Adequate to identify moderate level of degradation; incapable of identifying subtle degradation
Rudder deflection	34,800	0.005	Capable of predicting severe to moderate degradation
Pitch attitude	51,300	0.004	Capable of predicting moderate degradation
Bank angle	46,000	0.006	Capable of predicting severe to moderate degradation

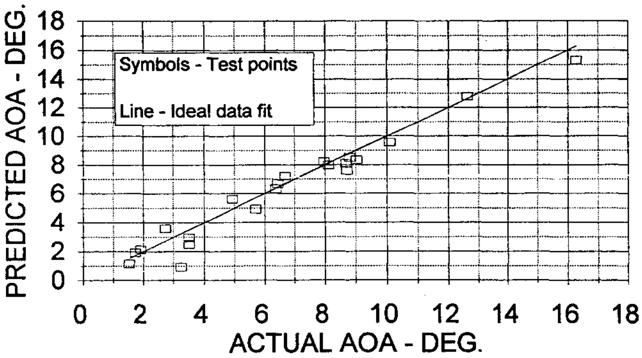

Fig. 4 Performance of the network for angle of attack from flight test data (network topology 12-5-5-1).

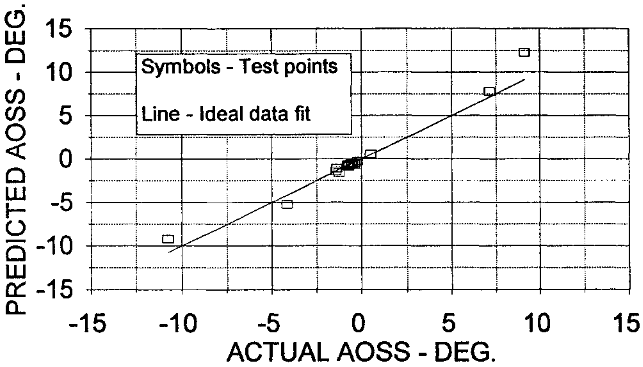

Fig. 5 Performance of the network for sideslip angle from flight test data (network topology 12-5-5-1).

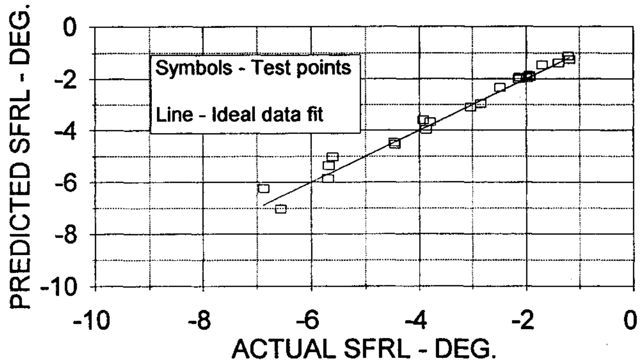

Fig. 6 Performance of the network for stabilizer incidence from flight test data (network topology 12-5-5-1).

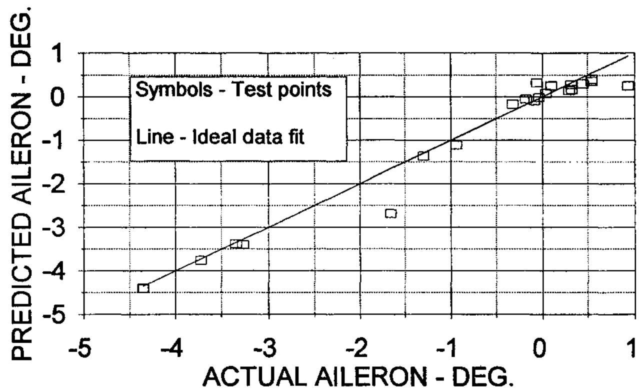

Fig. 7 Performance of the network for aileron deflection angle from flight test data (network topology 12-5-5-1).

suffered in varying degrees from the lack of sufficient training data in the moderate to high range of sideslip angle. However, the data used in this study were collected from a test program that was completed some time ago and, therefore, the option of acquiring more data was not available. A fundamental part of this research was to use actual flight data in ANN development. The quantity of data available from this test program was not adequate to achieve desired network performance in all cases. Therefore, it is concluded that for this system to be implemented and function properly future flight programs should include additional test points for network training. Depending on the length of the flight test program, the additional time spent collecting these data would be cost effective because 1) the number of flights repeated due to instrumentation failures would be reduced and 2) time spent reviewing data would be cut significantly. The tradeoff between adding test points for network training and saving repeat flights due to failures would have to be assessed for each flight program.

Figures 4–11 graphically illustrate the performance achieved by each network. In the interest of brevity, training results have been omitted here. The interested reader is advised to consult Ref. 15 for the training results. However, it should be mentioned that due to noise and other uncertainties, there existed some scatter in the training data from flight tests. Therefore, some of the errors in the following results are actually due to impurity of the training data.

1) Angle of attack: the results for angle of attack are shown in Fig. 4. This figure indicates good agreement between the actual flight test values and the network predicted values. All but one of the test conditions were predicted within approximately ± 1 deg and most are within ± 0.5 deg.

2) Sideslip angle: as indicated earlier, performance of the network for sideslip angle was restricted by the limited number of training sets with significant sideslip angle. Nevertheless, this network also performed reasonably well as shown

in Fig. 5. The training data was matched in this case to within approximately ± 0.5 deg. However, the test case indicated moderate scatter of approximately ± 1.0 deg, except at higher slip angles.

3) Stabilizer incidence angle: one of the best set of results was obtained in the case of stabilizer incidence angle. This network was able to learn the training data set within ± 0.25 deg and the test cases within approximately ± 0.5 deg as indicated in Fig. 6.

4) Aileron deflection angle: for this parameter there were differences between the results obtained from the network for simulation and that for flight test data. The performance of the simulation network was poor, whereas the flight test network showed that all of the training conditions and all but three of the test conditions were identified within ± 0.5 deg, as shown in Fig. 7. This result was attributed to the slight asymmetry present in a production aircraft, unlike the simulation model. This resulted in a small, but measurable aileron deflection to trim the aircraft in roll, thereby providing the training data with which to identify the system mapping.

5) Spoiler deflection angle: this network performed well considering the limited number of available sideslip cases. The training set was predicted within ± 1.0 deg and the test set within ± 2.0 deg for all but one case, as shown in Fig. 8.

6) Rudder deflection angle: the network trained for the identification of rudder deflection performed well on the training data set with errors ranging from ± 0.5 to ± 1.0 deg. However, this network failed to properly predict the test conditions, as indicated in Fig. 9. This was most likely due to the limited number of training cases with significant rudder deflection and the subsequent skewing of the network fit toward the symmetric trim conditions.

7) Pitch attitude: the performance of the pitch attitude ANN showed more scatter in the test cases than would be acceptable

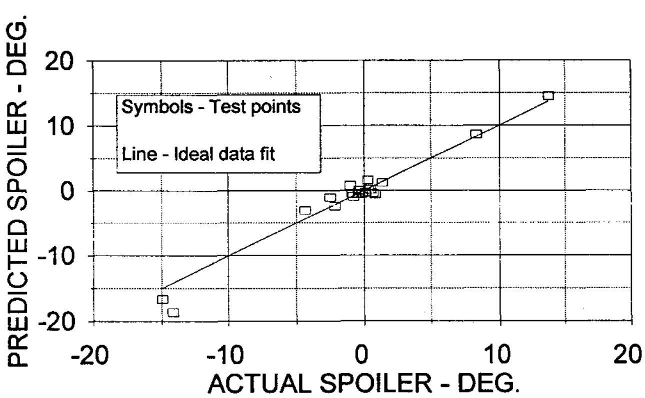

Fig. 8 Performance of the network for spoiler deflection angle from flight test data (network topology 12-5-5-1).

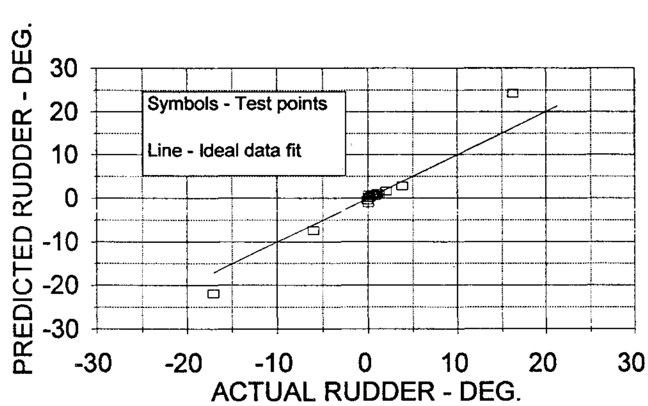

Fig. 9 Performance of the network for rudder deflection angle from flight test data (network topology 12-5-5-1).

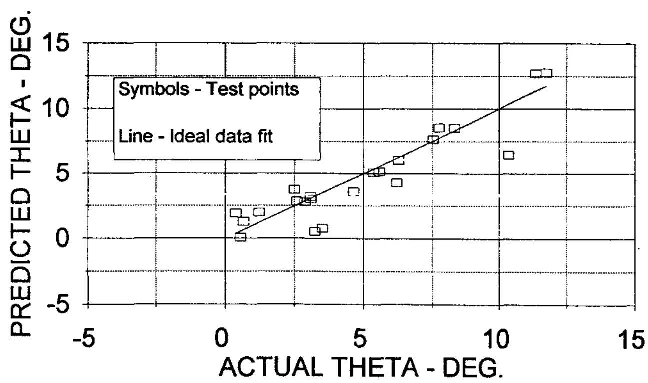

Fig. 10 Performance of the network for pitch attitude from flight test data (network topology 12-5-5-1).

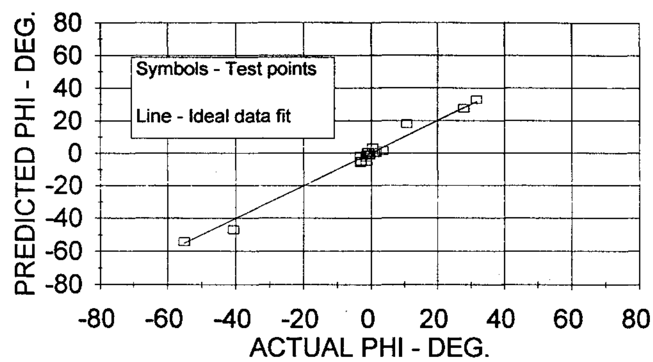

Fig. 11 Performance of the network for bank angle from flight test data (network topology 12-5-5-1).

for identification of subtle degradation in the instrumentation. This is clearly indicated in Fig. 10. This behavior may be attributed partly to the presence of the self-alignment mechanism in the pitch indicating gyroscope. This shortcoming of this type of gyroscope is well known, but may be acceptable on certain test programs. The use of this mechanism in this flight test program was not the preferred choice, however, it was unavoidable.

8) Bank angle: bank angle was predicted with moderate accuracy, but the ANN was again handicapped by the lack of training data with significant sideslip angles. The training data was predicted within ± 2.0 deg. The test data shown in Fig. 11 indicates errors ranging from ± 5.0 to ± 7.0 deg. This is adequate to detect significant degradation or failure of the gyroscope, but not sufficient to act in the capacity of identifying slow degradation.

IV. Conclusions

The potential for ANNs to identify instrumentation degradation during a flight test program was demonstrated. A summary of the findings from this research is listed next.

1) The original system identification task had to be broken into smaller subtasks, from one network identifying all 8 parameters to eight networks each mapping one parameter. This was required because the original network for the identification of all suspect instrumentation parameters did not perform adequately. The result of this task subdivision was a more accurate prediction capability of the resulting networks. Because these networks were smaller, the number of training cycles as well as the training time were reduced.

2) The resulting networks, trained with flight data, adequately predicted suspect instrument parameter outputs in 6 out of 8 cases, the exceptions being rudder deflection angle and bank angle. The network performance for predicting lateral-directional output parameters was restricted by the availability of limited training data in the higher range of sideslip

angle. This problem can be remedied by a collection of additional test points in the course of an ongoing flight test program.

3) These networks are practical because they provide a general modeling tool that does not require special knowledge of aircraft system identification schemes. The only requirement here is a minimum set of instrumentation inputs for proper network training and operation.

4) The method suggested here can easily be implemented in programmable hardware for use in real-time monitoring of an aircraft instrumentation data package.

5) This scheme lends itself well to test programs of longer duration where the flight time necessary to collect sufficient data for network training is a relatively small part of the overall program. In shorter flight test programs, the tradeoff in cost between additional time taken for data collection and that required for data analysis would have to be assessed.

6) Implementing a system using ANNs has some limitations. The choice of network topology is still a matter of trial and error. There are no formulas for making this choice. This became evident by the fact that several network topologies had to be tested in the simulation phase before arriving at a suitable configuration.

The findings from this research can be developed further. Additional work in the development of this system could include the following.

1) Determining the minimum number and optimum mixture of training cases to arrive at a proper mix of flight test types. This would assure adequate network training.

2) Experimenting with the minimum number of trusted instrumentation parameters required for adequate network performance.

3) Extending the method to monitor additional instrumented parameters such as engine interturbine temperature, etc.

4) Examining the effects of losing one or more of the trusted parameters; i.e., the possibility of the failure of one of the trusted parameters remaining undetected and jeopardizing the operation of the health monitoring system.

Furthermore, the only neural network architecture used in this study was that of a multilayer perceptron. It is possible that other paradigms such as radial basis function networks or generalized regression neural networks may yield better modeling for some of the suspect flight parameters. This would be the next logical step toward developing this into a usable flight test data system.

Acknowledgment

The authors wish to acknowledge Raytheon Aircraft Company for providing the flight test data for this research.

References

[1]Nguyen, D. H., and Widrow, B., "Neural Networks for Self-Learning Control Systems," *IEEE Control Systems Magazine*, Vol. 10, No. 3, 1990, pp. 18–23.

[2]Narendra, K. S., and Parthasarathy, K., "Identification and Control of Dynamical Systems Using Neural Networks," *IEEE Transactions on Neural Networks*, Vol. 1, No. 1, 1990, pp. 4–27.

[3]Levin, A. U., and Narendra, K. S., "Control of Nonlinear Dynamical Systems Using Neural Networks: Controllability and Stabilization," *IEEE Transactions on Neural Networks*, Vol. 4, No. 2, 1993, pp. 192–206.

[4]Huang, S. Y., Miller, L. S., and Steck, J. E., "An Exploratory Application of Neural Networks to Airfoil Design," AIAA Paper 94-0501, Jan. 1994.

[5]Faller, W. E., Schreck, S. J., and Luttges, M. W., "Real-Time Prediction and Control of Three-Dimensional Unsteady Separated Flow Fields Using Neural Networks," AIAA Paper 94-0532, Jan. 1994.

[6]Rokhsaz, K., and Steck, J. E., "Use of Neural Networks in Control of High Alpha Maneuvers," *Journal of Guidance, Control, and Dynamics*, Vol. 16, No. 5, 1993, pp. 934–939.

[7]Rokhsaz, K., Steck, J. E., and Shue, S. P., "Longitudinal Flight Control Decoupling Using Artificial Neural Networks," AIAA Paper 94-0274, Jan. 1994.

[8]Guo, T. H., and Musgrave, J., "A Neural Network-Based Estimator for the Mixture Ratio of the Space Shuttle Main Engine," NASA TM-106070, Nov. 1992.

[9]Hoyt, W. A., and Whitehead, B. A., "Automated Screening of Propulsion System Test Data by Neural Networks," NASA CR-184329, April 1992.

[10]Decker, A. J., and Weiland, K. E., "Calibration of a Shock Wave Position Sensor Using Artificial Neural Networks," NASA TM-106138, May 1993.

[11]Chiang, C. Y., Juang, J. C., and Youssef, H. M., "Neural Network Approach to Aircraft Fault Detection, Isolation, and Estimation Design," AIAA Paper 94-0273, Jan. 1994.

[12]Hess, R. A., "On the Use of Back Propagation with Feed-Forward Neural Networks for the Aerodynamic Estimation Problem," *AIAA Atmospheric Flight Mechanics Conference* (Monterey, CA), AIAA, Washington, DC, 1993, pp. 233–245 (AIAA Paper 93-3638).

[13]Youssef, H. M., and Juang, J. C., "Estimation of Aerodynamic Coefficients Using Neural Networks," AIAA Paper 93-3639, *AIAA Atmospheric Flight Mechanics Conference* (Monterey, CA), AIAA, Washington, DC, 1993, pp. 242–245 (AIAA Paper 93-3639).

[14]Iorgulescu, D. T., "Rapid Post-Flight Analysis System," AIAA Paper 94-0399, Jan. 1994.

[15]McMillen, R. L., "Application of an Artificial Neural Network as a Flight Test Data Estimator," M.S. Thesis, Dept. of Aerospace Engineering, Wichita State Univ., Wichita, KS, 1994.

[16]Thelander, J. A., "Aircraft Motion Analysis," Air Force Flight Dynamics Lab., FDL-TDR-64-70, March 1965.

[17]Gainer, T. G., and Hoffman, S., "Summary of Transformation Equations and Equations of Motion Used in Free-Flight and Wind-Tunnel Data Reduction and Analysis," NASA SP-3070, 1972.